ISSN 2321-807X
Volume 12 Number15
Journal of Advances in chemistry

VIBRATIONAL SPECTRA, NBO, HOMO-LUMO ANALYSES OF FURFURAL SEMICARBAZONE

Dr.R.Kumutha[1], Dr.S.Sampath Krishnan*[2]
[1]Department of Physics, S.A Engineering College, Chennai
kumuthar@saec.ac.in
[2]Department of Physics, Sri Venkateswara College of Engineering, Sriperumbadur, Chennai - 602117
sambathk@svce.ac.in
*Corresponding author e-mail: sambathk@svce.ac.in Tel:9444245284

ABSTRACT

The molecular structure and vibrational spectra of Furfural Semicarbazone (FSC) have been calculated with the help of density fuctional theory (DFT) using 6-31++G(d,p) and 6-311++G(d,p) basis sets. The solid phase FT-IR and FT-Raman spectra of furfural semicarbazone have been recorded in the range 4000-400cm^{-1} and 4000-100 cm^{-1}, respectively. On the basis of B3LYP calculations, the normal coordinate analysis has been performed to assign the vibrational fundamental frequencies according to potential energy distribution. The optimum molecular geometry, harmonic vibrational frequencies, infrared intensities and Raman Scattering activities were calculated by density functional theory (DFT/B3LYP) method with 6-31++G(d,p) and 6-311++G(d,p) basis sets. The difference between the observed and scaled wave number values of most of the fundamentals is very small. Stability of the molecule arising from hyper conjugative interactions, charge delocalization have been analyzed using Natural Bond Orbital (NBO) analysis. The electro dipole moment (μ) and first hyperpolarizability (β) values of the investigated molecule are computed using Scaled Quantum Mechanical Force field (SQMF) method. Besides, HOMO and LUMO analysis and Fukui functions of the title molecule have also been calculated using DFT method.

Indexing terms/Keywords

DFT, Natural Bond Orbital (NBO) analysis, HOMO and LUMO, Fukui functions

Academic Discipline And Sub-Disciplines

Applied Physics

SUBJECT CLASSIFICATION

Physics Subject Classification; Spectroscopy

TYPE (METHOD/

Quantum Chemical Calculation – DFT studies

INTRODUCTION

A number of aliphatic and aromatic semicarbazone derivatives have been prepared by the condensation of a variety of ketones with semicarbazide. The products have been characterized by analytical and spectral methods. The semicarbazone derivatives were screened for anti-bacterial activity by diffusion method, using nutrient agar medium and some of the products have shown biological activities against common test organisms. Recently some workers had reviewed the bioactivity Rouse et al (2003) activities. Accordingly and by considering the biological potential of semicarbazones.

Extensive work has been done with the structure analogues of semicarbazone, and may have been found to exhibit interesting biological and chemotherapeutic properties. The spectroscopic studies of semicarbozone and its derivatives have been motivated by their occurrence in natural biological systems Kupchan et al (1974), Georgieva et al (2006) although free molecules do not occur in biological systems. The understanding of the vibrational spectra of free base molecules would be very useful for the understanding of specific biological processes and in the analysis of relatively complex system

SYNTHESIS

1 gram of semicarbazide hydrochloride and 1.5 gram of sodium acetate were dissolved in 10 ml of water. 0.5 gram of the furfural was added to the above mixture. The mixture was stirred for a few minutes and allowed to stand. Furfural semicarbazone crystallized out from solution on standing. The crystals were filtered, washed with cold water and recrystallised from water. The scheme of the synthesis is shown in Figure 1.

ISSN 2321-807X
Volume 12 Number15
Journal of Advances in chemistry

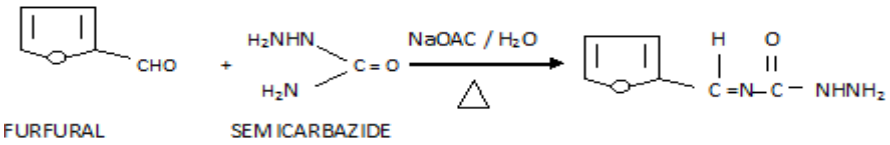

Figure 1 The scheme of the synthesis of FSC

EXPERIMENTAL DETAILS

The fourier transform infrared spectra of the title compound was recorded in the region 4000-400 cm^{-1}, using Bracker IFS 66V model FT-IR Spectrometer equipped with an MCT detector, a KBR beam splitter and globar source. The spectral resolution is ± cm^{-1}.

The FT-Raman Spectrum of FSC was recorded on a computer interfaced BRUCKER IFS 66V model interferometer equipped with FRA-106 FT-Raman accessories. The spectrum was measured in the region 4000-100 cm^{-1} using Nd:YAG laser operating at 200 mW power continuously with 1064 nm excitation. The spectra were recorded with scanning speed of 30 cm^{-1} min^{-1} of spectral width 2 cm^{-1}. The frequencies of all sharp bands are accurate to ±1 cm^{-1}.

COMPUTATIONAL DETAILS

In the frame work of DFT approach, different exchange and correlation functions were routinely used. Among these, the B3LYP combination (Becke 1993) is the most used since it proved its ability in reproducing various molecular properities, including vibrational spectra. In order to provide information with regard to the structural characteristics and the normal vibrational modes of FSC, the DFT-B3LYP correlation functional calculations have been carried out. The molecular geometry optimizations, energy and vibrational frequency calculations were carried out for FSC with the GAUSSIAN 03W software package. The DFT level calculations, employing the B3LYP keyword, which invokes Becke's three parameter hybrid method Pulay et al (1983), Fogarasi & Pulay (1985), (Sundius 2002) has been computed using the correlation function of Lee et al (1998), implemented with 6-31++G(d,p) and 6-311++G(d,p) basis sets. All the parameters were allowed to relax and all the calculations converged to an optimized geometry which corresponds to a true minimum, as revealed by the lack of imaginary values in the wavenumber calculations. The Cartesian representation of the theoretical force constants have been computed at optimized geometry by assuming C_1 point group symmetry. Scaling of the force field was performed according to SQMF procedure Pulay et al (1983), Fogarasi & Pulay (1985) using selective scaling in the natural internal coordinate representation Fogarasi & Pulay (1985). Normal coordinate analysis has been performed to obtain full description of the molecular motion pertaining to the normal modes with MOLVIB program version 7.0 written by Sandius (2002). For plots of simulated IR spectra, pure Lorentizian band shapes were analysed with a band width (FWHM) of 10 cm^{-1}. The Raman intensities (δ_i) calculated by Gaussian 03W program have been suitably adjusted by the scaling procedure with MOLVIB and subsequently converted to relative Raman intensities (I_i) using the following relationship derived from the basis theory of Raman scattering.

$$I_i = f (v_o - v_i)^{4\delta i} / v_i (1-\exp (hcv_i / k_b T) \quad (1)$$

Where is the exciting frequency in cm^{-1}, v_i the vibration wave number of the i^{th} normal mode, h, c and k_b are the fundamental constants and f is a suitably chosen common normalization factor for the entire peak intensities Olszak et al (1995). The simulated IR and Raman spectra have been plotted using Lorentizian shapes with Full Width at Half Maximum (FWHM) of 10 cm^{-1}. Natural Bond Orbital (NBO) analysis Molvib (v.7.0), Keresztery et al (2002), Glendering et al (1998) has been performed using NBO 3.1 program as implemented in the Gaussian 03W package at the DFT/B3LYP/6-31++G(d,p) level of theory.

RESULT AND DISCUSSION

Molecular Geometry

The optimized molecular structure with the numbering of atoms of the title compound is shown in Figure 1.2. The most optimized structural parameters are also calculated by B3LYP method with 6-31++G(d,p) and 6-311++G(d,p) as basis sets and they were presented in Table 1 they were presented in Table 1.The calculated values were compared with X-ray diffraction results. From the structural data given in Table 1. Table compares with those of experimental data Klots et al (1994), one can find that most of the optimized bond lengths are larger than experimental values. This is due to the fact that the theoretical calculations result from isolated molecules in gaseous phase while the experimental results are from molecules in solid state. Comparing bond angles and bond lengths of B3LYP/ 6-31++G (d,p) and 6-311++G (d,p) basis set for FSC, it is also observed that the geometrical parameters were found to be almost same at both levelsThe calculated C-C bond length of the Furan ring vary from 1.36 to 1.42 Å calculated by B3LYP/6-311++G (d, p) method. The C(1)-C(2) bond length is 1.442 Å. This is larger than the C-C bond distance of the furan ring. This clearly shows that there is no delocalization of the π- electrons of N=C towards the ring of FCS. The calculated furan ring bond angle by B3LYP/6-31++G (d, p) and 6-311++G(d,p) basis sets lies in the range 106.55° to 110.64°. The bond angle of C(1)-C (2)-O(6) and C(3)-C(2)-O(6) are equal to 119.59° and 109.61°, respectively. This variation of the bond angle depends on the electro negativity of the central atom. If the electro negativity of the central atom increases, bond angle increases.

ISSN 2321-807X
Volume 12 Number15
Journal of Advances in chemistry

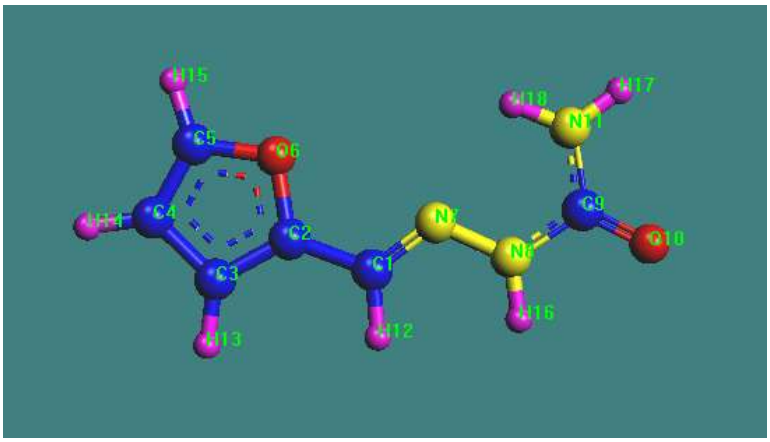

Figure 2 Molecular Structure of FSC with numbering of atoms

Detailed description of vibrational modes can be given by means of normal coordinate's analysis. For this purpose the full set of 48 standard internal coordinates were analysed. For the title compound are defined in Table 2. From these, a non-redundant set of local symmetry coordinates were constructed by suitable linear combinations of internal coordinates following the recommendations of Fogarasi & Pulay (1985) which are summarized in Table 3

Table 1 Optimized geometrical parameters for FSC with different basis sets

Parameters	B3LYP/ 6-31++G(d,p)	B3LYP/ 6-311G++(d,p)	Experimental*
BOND LENGTH			
C(1)-C(2)	1.4417	1.4402	1.462
C(1)-N(7)	1.2882	1.2836	1.2599
C(1)-H(12)	1.0958	1.0942	1.080
C(2)-C(3)	1.3754	1.3714	1.369
C(2)-O(6)	1.3682	1.3657	1.373
C(3)-C(4)	1.4292	1.4279	1.4259
C(3)-H(13)	1.0809	1.0787	1.081
C(4)-C(5)	1.3648	1.3605	1.368
C(4)-H(14)	1.0804	1.0781	1.1
C(5)-O(6)	1.3629	1.3606	1.353
C(5)-H(15)	1.0788	1.0769	1.1
N(7)-N(8)	1.3523	1.3497	1.352
N(8)-C(9)	1.3957	1.3971	1.215
N(8)-H(16)	1.0172	1.0159	1.012
C(9)-O(10)	1.2276	1.2194	1.208
C(9)-N(11)	1.36	1.3588	1.309
N(11)-H(17)	1.0062	1.0047	1.0119
N(11)-H(18)	1.0087	1.0074	1.012
BOND ANGLE			
C(2)-C(1)-N(7)	122.50	120.55	119.99
C(2)-C(1)-H(12)	115.51	115.43	119.99
N(7)-C(1)-H(12)	121.98	122.01	125.91
C(1)-C(2)-C(3)	130.80	130.70	128.49

C(1)-C(2)-O(6)	119.59	119.64	111.04
C(3)-C(2)-O(6)	109.61	109.64	105.85
C(2)-C(3)-C(4)	106.55	106.52	109.97
C(2)-C(3)-H(13)	126.04	126.06	126.58
C(4)-C(3)-H(13)	127.41	127.42	127.561
C(3)-C(4)-C(5)	106.03	106.03	106.33
C(3)-C(4)-H(14)	127.49	127.52	133.39
C(5)-C(4)-H(14)	126.49	126.44	126.02
C(4)-C(5)-O(6)	110.64	110.66	110.93
C(4)-C(5)-H(15)	133.62	133.54	133.39
O(6)-C(5)-H(15)	115.74	115.80	116.87
C(2)-O(6)-C(5)	107.18	107.15	106.90
C(1)-N(7)-N(8)	118.21	118.42	119.09
N(7)-N(8)-C(9)	121.97	122.07	123.03
N(7)-N(8)-H(16)	122.41	122.31	124.05
C(9)-N(8)-H(16)	115.62	115.62	115.66
N(8)-C(9)-O(10)	119.90	120.02	120.00
N(8)-C(9)-N(11)	114.86	114.51	114.56
O(10)-C(9)-N(1)	125.23	125.48	125.78
C(9)-N(11)-N(17)	117.68	117.80	117.99
C(9)-N(11)-H(18)	120.93	120.77	120.23
H(17)-N(11)-H(18)	121.39	121.43	120.53

Table 2 Definition of internal coordinates of FSC

No.	Type	Definition
Stretching (r_i)		
1-3	O-C	C2-O6, C5-O5, C9-C10
4-7	C-C	C1-C1, C2-C3, C3-C4, C4-C5
8-10	C-N	C9-N8, C1-N7, C9-N11
11-14	C-H	C3-H13, C4-H14, C5-H15, C1-H12
15-17	N-H	N8-H16
	NH_2	NH_2(sym), NH_2(asym)
In-Plane Bending(β_i)		
18-22	Ring	O6-C2-C3, C2-C3-C4, C3-C4-C5, C4-C5-O6, C5-O6-C2
23	C-C-C	C3-C2-C1
24	O-C-C	C3-C2-O6
25	C-C-N	C2-C1-N7
26-28	C-N-N	C1-N7-N8, C9-N8-N7, N8-C9-N11
29-30	N-C-O	N8-C9-O10, N11-C9-O10
31	N-N-H	N7-N8-H16
32-33	C-N-H	C9-N8-H16, C1-N7-H12

34-39	C-C-H	C1-C2-H12, C2-C3-H13, C4-C3-H13, C3-C4-H14, C4-C5-H14, C4-C5-H15
40	O-C-H	O6-C5-H15
41	N-H-H	N11-H17-N18
Out-of- Plane Bending (v_i)		
42	C-C	C1-C2-C3-O6
43-46	C-H	C4-C5-O6-H15, C3-C4-C5-H14, C1-C2-C3-H13, C1-C2-C3-H12
47-48	N-H	C1-N7-N8-H16, N7-N8-C9-H16
49	N-O	N8-C9-N11-O10
50	C-N	C9-N11-H17-H18
Torsion(τ)		
51-55	T_{ring}	O6-C2-C3, C2-C3-C4, C3-C4-C5, C4-C5-C6, C5-O6-C2
56	T_{C-NH2}	C9-N11-H17-H18

Table 3 Definition of local symmetry coordinates in B3LYP/6-31++G (d,p) for FSC

S.No	Symmetry Coordinates	Description
1	$S_1 = r_{12}$	vC_1C_2
2.	$S_2 = r_{17}$	$v\ C_1N_7$
3.	$S_3 = r_{112}$	vC_1H_{12}
4.	$S_4 = r_{23}$	vC_2C_3
5.	$S_5 = r_{26}$	vC_2O_6
6.	$S_6 = r_{34}$	vC_3C_4
7.	$S_7 = r_{313}$	$vC_3\ H_{13}$
8.	$S_8 = r_{45}$	$v\ C_4C_5$
9.	$S_9 = r_{56}$	$v\ C_5O_6$
10.	$S_{10} = r_{515}$	$v\ C_5H_{15}$
11.	$S_{11} = r_{78}$	$v\ N_7N_8$
12.	$S_{12} = r_{89}$	$v\ N_8C_9$
13.	$S_{13} = r_{816}$	$v\ N_8H_{16}$
14.	$S_{14} = r_{910}$	$v\ C_9O_{10}$
15.	$S_{15} = r_{911}$	$v\ C_9N_{11}$
16.	$S_{16} = r_{1117}$	$v\ N_{11}H_{17}$
17.	$S_{17} = r_{1118}$	$v\ N_{11}H_{18}$
18.	$S_{18} = \beta_{2313} - \beta_{4313}$	βC_3H_{13}
19.	$S_{19} = \beta_{3\,4\,14} - \beta_{5\,4\,14}$	βC_4H_{14}
20.	$S_{20} = \beta_{4\,5\,15} - \beta_{6\,5\,15}$	βC_4H_{15}
21.	$S_{21} = \beta_{7\,8\,16} - \beta_{9\,8\,16}$	βN_8H_{16}
22.	$S_{22} = \beta_{8\,9\,11} - \beta_{10\,9\,11}$	βC_9N_{11}
23.	$S_{23} = \beta_{9\,11\,18} - \beta_{17\,11\,18}$	$\beta N_{11}H_{18}$
24.	$S_{24} = \beta_{2\,1\,12} - \beta_{7\,1\,12}$	βC_1H_{12}
25.	$S25 = \beta\ 18\ 11\ 9 - \beta\ 7\ 11\ 9$	βN11C9
26.	$S26 = \beta\ 2\ 6\ 5 + a(\beta\ 6\ 5\ 4 + \beta\ 3\ 2\ 6) + b(\beta\ 2\ 3\ 4 + \beta\ 4\ 5\ 6)$	β ring

27.	S27 = υ1 2 6 3	υ C1C2
28.	S28 = υ13 3 2 4	υ C3H13
29.	S29 = υ14 4 5 3	υ C4H14
30.	S30 = υ15 5 4 6	υ C5H15
31.	S31 = υ12 1 7 2	υ C1H12
32.	S32 = υ10 8 9 7	υ N8H16
33.	S33 = υ9 11 17 18	υ C9N11
34.	S34 = b(υ5 6 2 3+ υ2 3 4 5)+a(υ6 5 4 3+ υ4 3 2 6)+ υ3 2 6 5	υ ring
35.	S35 = τ 13 3 4 14	τ H13C3
36.	S36 = τ 14 4 5 15	τ H14C4
37.	S37 = τ 12 1 2 3	τ H12C1
38.	S38 = τ 16 8 7 1	τ H16N8
39.	S39 = τ 10 9 8 16	τO10C9
40.	S40 = τ 11 17 9 10	τN11H17
41.	S41 = τ 1 2 3 13	τ C1C2
42.	S42 = τ 7 1 2 6	τ N7C1
43.	S43 = τ 8 9 11 18	τ N8C9
44.	S44 = τ 2 6 5 15	τ C2O6
45.	S45 = τ 5 4 3 13	τ C5C4
46.	S46 = τ 2 3 4 14	τ C2C3
47.	S47 = τ 7 8 9 10	τ N7N8
48.	S48 = τ 14 4 5 6 + τ 13 3 4 14 + τ 15 5 6 2	τ CH

Vibrational Assignments

The molecule FSC belongs to C_1 point group symmetry and its 48 fundamental modes of vibrations. All these modes are found to be active both in the Raman scattering and infrared absorption.

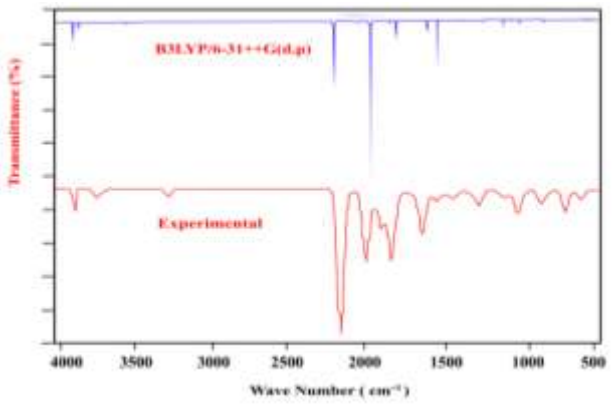

Figure 3 Comparison of experimental and computed FT-IR spectra of FSC

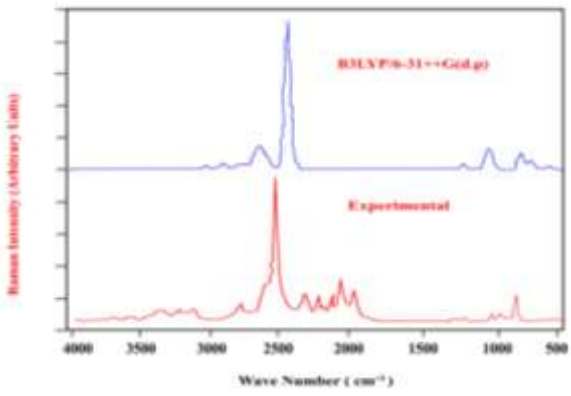

Figure 4 Comparison of experimental and computed FT-Raman spectra of FSC

The detailed vibrational assignments of fundamental modes of FSC along with the calculated IR and Raman frequencies and normal mode descriptions are reported in Table 4.

Table 4 Experimental and B3LYP levels computed vibrational assignments of FSC

Mode N.	Experimental frequency cm^{-1}		Theoretical Values cm^{-1}		B3LYP/6-31++G(d,p)		B3LYP/6-311+G(d,p)		Assignments
	FT-IR	FT-RAMAN	B3LYP/ 6-31++G(d,p)	B3LYP/ 6-311+G(d,p)	[a]IR Intensity	[b]Raman Intensity	[a]IR Intensity	[b]Raman Intensity	
1	3456(s)	-	3476	3459	15.08	17.06	14.77	20.47	νNH_2(asy)(98)
2	3342(vs)	3366(s)	3351	3352	5.34	42.82	5.08	52.28	νNH_2(sym)(99)
3	3280(m)	3171(ms)	3295	3281	1.91	82.82	1.95	100.00	νNH(99)
4	3095(s)	3077(w)	3070	3048	0.01	51.65	0.02	63.29	νCH(96)
5	2998(w)	-	3045	3024	0.05	37.36	0.02	42.07	νCH(92)
6	2996(s)	-	3033	3013	0.65	36.07	0.61	43.52	νCH(98)
7	2977(ms)	2962(ms)	2959	2938	4.74	26.81	4.44	32.94	νCH(99)
8	1857(vs)	1843(ms)	1814	1809	100.00	41.07	100.00	49.16	νOC(69), νNC(10)
9	1689(vs)	-	1624	1611	2.02	68.68	2.14	88.87	νN=C(57), νCC(14),βHCN(12)
10	1658(m)	1628(vw)	1646	1636	5.76	0.46	6.42	0.65	νN=C(15), νCC(18),νCC(32)
11	1601(vw)	1611(w)	1584	1588	45.49	11.33	39.44	14.84	βNH_2(85)
12	1519(ms)	1557(w)	1473	1464	8.24	57.32	7.39	57.98	νCC(56), βHNN(13), βHCO(10)
13	1473(vs)	1473(ms)	1421	1415	24.92	100.00	18.00	130.66	νCC(40), βHNN(37)
14	1456(vs)	-	1376	1365	1.39	68.98	2.01	85.89	βCOO(10), βHCC(22), βHCO(14), βCCO(21)
15	1418(vw)	1392(s)	1349	1340	47.13	1.97	50.74	1.30	νCC(32), νNC(16),βHNC(14), βOCN(13)
16	1332(vs)	1332(ms)	1299	1294	4.09	17.96	5.78	27.26	νCN(58)
17	1278(vs)	1279(s)	1255	1243	0.49	22.77	0.44	25.22	νCC(20), νOC(28),βCCO(11)
18	1220(s)	1223(s)	1202	1194	3.47	6.62	3.27	6.71	βHCC(41), βHCO(18)
19	1156(ms)	1154(ms)	1143	1134	6.59	7.77	12.13	16.59	βHCO(32),νOC(17), νNN(20),
20	1139(w)	1139(w)	1129	1120	24.89	22.28	19.19	23.04	νOC(16), νNN(39)
21	1120(s)	1118(w)	1065	1058	0.52	4.54	0.47	5.39	νCC(10), νOC(38),βCCO(16)
22	1098(vw)	1073(s)	1044	1044	6.07	1.73	8.37	1.51	δNH_2(73),βHCN(34)
23	1010(vs)	1026(w)	1003	996	3.94	16.05	3.84	21.65	βHCC(31), βCOC(16)

24	998(ms)	1012(vs)	957	951	1.94	2.34	2.01	2.66	γHCC(38),νNC(24),βNCC(19)
25	947(w)	-	914	911	3.38	3.87	3.51	5.47	γHCC(34),νCC(12), βCCO(11)
26	930(s)	931(w)	895	896	2.16	2.46	1.93	2.90	γHCN(46)
27	-	908(vw)	863	867	1.85	3.70	1.66	4.53	βCCO(61), βCOC(21)
28	883(ms)	884(ms)	847	847	0.00	0.72	0.00	0.93	τHCCC(22), τHCCO(17), τHCOC(15)
29	812(vw)	-	783	783	1.78	0.56	1.66	0.43	τHCOC(19)
30	803(ms)	789(w)	765	765	1.01	3.18	1.06	4.38	βNCC(38), βCCO(15)
31	751(s)	-	722	724	9.97	1.03	1.70	0.07	ωNH_2(66)
32	739(vs)	724(vw)	715	720	1.33	0.03	9.17	0.89	τHCCO(34)
33	656(ms)	-	654	655	0.04	0.40	0.05	0.53	τCCOC(26), ωCCOC(31)
34	644(s)	623(w)	611	611	0.01	0.78	0.01	0.93	νNC(50), βNCC(40), βNCN(23)
35	595(vs)	598(vw)	578	579	1.23	0.11	1.25	0.11	τHCOC(11),τCCOC(15)
36	575(vw)	573(w)	563	560	0.74	0.11	0.48	0.10	τHNCN(38)
37	531(ms)	526(vw)	529	532	5.05	1.16	4.90	1.41	βOCN(65)
38	461(s)	412(ms)	449	444	13.66	0.23	13.70	0.33	τHNNC(27)
39	418(vw)	403(vs)	423	424	4.44	1.22	4.25	1.53	τNH_2(48),βCCO(25), βNNC(11),
40	347(vs)	372(vw)	352	350	0.56	0.32	0.60	0.50	τNNCC(27),τCCOC(16),ωCCOC(12)
41	321(w)	-	305	304	0.25	0.99	0.27	1.20	νCC(20), νNC(13),βNNC(22)
42	-	269(ms)	270	272	10.07	0.55	9.52	0.64	τNCCC(17),τNCNN(27),τCNNC(13),ωCCOC(13)
43	202(w)	201(ms)	214	215	1.88	0.70	1.82	0.85	βNCN(16), βCCO(34), βCNN(30),
44	-	152(ms)	129	125	0.01	0.14	0.07	0.17	τNCCC(24), τCNNC(21), ωCCOC(24)
45	111(w)	109(w)	99	93	15.40	0.07	11.72	0.07	τHNCN(25), τHCCC(18), τNNCC(15)
46	92(m)	90(w)	75	74	0.10	0.64	0.09	0.78	βNCC(35), βCCO(18),

									βNNC(24)
47	56(w)	-	52	50	0.04	0.50	0.01	0.65	τNCCC(38), τCNNC(21)
48	-	-	37	41	6.54	0.16	8.63	0.28	τHNCN(25), τNCNN(12)

Abbreviations: w-weak, vw- very weak, m- medium, s- strong, vs- very strong, υ- stretching, υ_{as}- asymmetric stretching, υ_s- symmetric stretching, β- in-plane bending, γ- out-of plane bending, ω-wagging and τ- torsion.

NH_2/NH vibrations

The NH_2 group gives rise to six internal modes, namely symmetric stretching-$\nu_s(NH_2)$, anti-symmetric stretching-$\nu_{as}(NH_2)$, scissoring (or) symmetric deformation (or) simply deformation-$\beta(NH_2)$, anti-symmetric deformation (or) rocking $\delta(NH_2)$, wagging–$\omega(NH_2)$,andtorsionortwist- τ (NH_2) modes. For FSC the ν_s, ν_{as}, τ and ω modes are usually localized and are pure group modes, whereas β and δ modes mix up with other ring modes Arivazhagan et al (2010). The calculated NH_2 asymmetric stretching vibrations give rise to the strong band at 3463, 3446 cm^{-1} compared to the experimental result at 3456 cm^{-1} Bambagiooti et al (1974). The theoretically observed NH_2 symmetric vibration give rise to the strong band at 3312,302 cm^{-1} compared to the experimental values at 3342 and 3366 cm^{-1} in FT-IR and FT Raman spectrum of FSC. The N-H groups show their stretching vibration in the region 3500-3220 cm^{-1}. The position of the absorption in this region depends upon the degree of hydrogen bonding and, upon the physical state of the sample (or) the polarity of the solvent. In the present work, the bands appear at 3280 cm^{-1} in the FT-IR and 3271 cm^{-1} in the FT-Raman. The theoretically observed NH symmetric stretching vibration gives rise to 3233 and 3222 cm^{-1}. The scissoring mode (β) of the NH_2 groups gives rise to its characteristic frequencies in the region 1600-1700 cm^{-1} which contains a broad and strong IR band with peak at 1601 cm^{-1} in FT-IR and 1611 cm^{-1} in FT Raman for FSC. The rocking δ (NH_2) mode usually appears in the region 900-1150 cm^{-1} for nucleic acid bases. In the present case the IR band at 1098 cm^{-1} is associated with this mode. In the assignment the $\omega(NH_2)$ and $\tau(NH_2)$ modes have been assigned at 751 cm^{-1} and 418 cm^{-1}.

C-H vibration

The heteroaromatic organic compounds and its derivatives are structurally very close to benzene and commonly exhibit multiple weak bands in the region 3100-3000 cm^{-1} Zinczuk et al (2009) due to C-H stretching vibration Rastogi et al (2002), Arivazhagan et al (2010). In our study, the FT-IR vibrational frequencies found at 3095, 2998, 2996 and 2977 cm^{-1} are assigned to C-H stretching vibration of FSC. The theoretically computed C-H vibrations by B3LYP/6-31++G(d,p) and 6-311++G(d,p) methods show good agreement with recorded spectrum as well as the literature data. The C-H in-plane and out-of-plane bending vibrations generally lie in the range1300-1000 cm^{-1} and 1000-750 cm^{-1}, respectively. The FT-IR band at 1220, 1156, 1098 and 1010 cm^{-1} and FT-Raman band 1223, 1154, 1073 and 1026 cm^{-1} are assigned to C-H in-plane bending vibration of FSC. The peaks at 998,947 and 930 cm^{-1} in FT-IR and 931 and 908 cm^{-1} confirm the C-H out- of- plane bending vibration which agrees with the above said literature values. In general, the C-H vibrations (stretching, in plane and out of plane bending vibrations) calculated theoretically are in good agreement with experimental values Klots et al (1994), Zhang et al (2011) .

C-N vibrations

The identification of C-N vibrations is a very difficult tasks, since mixing of several bands are possible in this region. Silverstein &Webster (1981) assigned C-N stretching absorption in this region 1382-1266 cm^{-1}, for aromatic amines. In this study the bands observed at 1332 cm^{-1} in IR have been assigned to C-N stretching vibration of FSC. The slight shift in wave number is due to the fact that force constants of the C-N bond increases due to resonance with the ring. Pyrimidine absorbs strongly in the region 1600-1500 cm^{-1} due to the C=C and C=N ring stretching vibrations (Dani 1995), Arivazhagan et al (2010). In FSC, the band observed at 1689 cm^{-1} in IR spectrum is assigned to C=N stretching vibration and the corresponding force constants contribute 87% to the Total Energy Distribution (TED). The C-N in- plane and out-of-plane bending vibrations have also been identified and are listed in Table 3.

Furan ring vibrations

Generally the C-C stretching vibrations in aromatic compounds from the band in the region of 1430-1650 cm^{-1} Zinczuk et al (2009). According to (Socrates 2001), the presence of conjugate substituent such as C=C causes a heavy doublet formation around the region 1625-1575 cm^{-1}. The six ring carbon atoms undergo coupled vibrations, called skeletal vibrations and give a maximum of four bands in the region 1660-1420 cm^{-1} (Kalsi 1993). Five membered ring hetero aromatic compounds with two double bond in the ring, generally shows three ring stretching bands near 1590,1490 and 1400 cm^{-1} Klots et al (1994), Zhang et al (2011). As predicted in the earlier references the prominent peaks at 1519/1557, 1473/1473, and 1418/1392 cm^{-1}in the FT-IR/ Raman spectra are assigned to C=C and C-C stretching vibrations for the title compound and these modes are supported by their TED values. Most of the ring vibrational modes are affected by the substitutions in the aromatic ring of the title compound. In the present study, the mode with major contribution from furan ring deformation is attributed at 883 and 812 cm^{-1} in Infrared spectrum and corresponds well with the calculated wave number. The peak observed at 526 cm^{-1} in Raman and 531 cm^{-1} in IR Spectrum are assigned to the furan ring torsional modes by careful consideration of their quantitative descriptions. The reductions in the frequencies of

these modes are due to the change in force constants and the vibrations of the functional groups present in the molecule. The theoretically computed values by B3LYP/6-311++G(d,p) method gives excellent agreement with experimental data.

Natural Bond Analysis (NBO)

NBO analysis is an efficient method for studying intra and intermolecular bonding and interaction among bond and also provides a convenient basis for investigating charge transfer or conjugate interactions in molecular systems. It was performed by using NBO 3.1 program implemented in the Gaussian 03W package at the DFT/B3LYP level in order to understand various second order interactions between the filled orbitals of one subsystem and vacant orbitals of another subsystem Read et al (1988), Choo et al (2002), which is a measure of the delocalization or hyperconjugation. NBO method gives useful information about the interactions in both filled and virtual orbital spaces. In this analysis large $E^{(2)}$ value shows the intensive interaction between electron donors and electron acceptors a greater extent of conjugation of the whole system. For each donor (i) and acceptor NBO (j) the stabilization energy $E^{(2)}$ associated with an electron delocalization between donor and acceptor is estimated as Luque et al (2000), Okulik & Jubert (2005):

$$E^{(2)} = \Delta E_{ij} = q_i \frac{F(i,j)^2}{\varepsilon_j - \varepsilon_i} \quad (2)$$

q^i = orbital occupancy

$\varepsilon_j - \varepsilon_i$ = diagonal elements

F(i,j) = off diagonal NBO Fock matrix element

Table 5 Second order perturbation theory analysis of Fock matrix in NBO basis of FSC

Donor(i)	Type	ED(e)	Acceptor(j)	Type	ED(e)	$E^{(2)a}$ (kJ/mol)	E(j)– E(i)[b](a.u.)	F(i, j)[c] (a.u.)
C_1-C_2	σ	1.9575	C_1-N_7	σ *	0.0107	4.08	1.14	0.068
			C_1-H_{12}	σ *	0.0368	0.75	1.12	0.026
			C_2-C_3	σ *	0.0277	7.18	1.39	0.089
			C_2-O_6	σ *	0.0326	3.28	1.29	0.058
			C_3-C_4	σ *	0.0124	1.06	1.39	0.034
			C_5-O_6	σ *	0.0154	2.97	1.29	0.055
			N_7-N_8	σ *	0.0238	4.88	1.15	0.067
C_1-N_7	σ	1.9861	C_1-C_2	σ *	0.0346	3.32	1.55	0.064
			C_1-H_{12}	σ *	0.0368	0.82	1.29	0.029
			C_2-C_3	σ *	0.0277	2.23	1.55	0.053
			N_8-C_9	σ *	0.0717	1.83	1.38	0.045
C_1-N_7	π	1.9282	C_1-N_7	π *	0.02763	0.50	0.36	0.013
			C_2-C_3	π *	0.3697	13.37	0.37	0.069
C_2-C_3	σ	1.9697	C_1-C_2	σ *	0.0346	8.15	1.36	0.094
			C_1-N_7	σ *	0.0107	1.85	1.39	0.045
			C_2-O_6	σ *	0.0326	1.80	1.27	0.043
			C_3-C_4	σ *	0.0124	3.20	1.37	0.059
			C_3-H_{13}	σ *	0.0210	1.36	1.14	0.035
			C_4-H_{14}	σ *	0.0126	1.69	1.13	0.065
C_9-O_{10}	σ	1.9910	N_7-N_8	σ *	0.0238	1.89	1.45	0.047
			N_8-C_9	σ *	0.0717	1.17	1.50	0.038
N_{11}-H_{17}	σ	1.9897	N_8-C_9	σ *	0.0717	4.33	1.11	0.063
			C_9-O_{10}	σ *	0.0112	0.54	1.32	0.024
O_6	LP_1	1.9495	C_1-C_2	σ *	0.0346	1.94	1.20	0.043
			C_2-C_3	σ *	0.0277	5.74	1.21	0.075

			C_4-C_5	σ *	0.0209	6.66	1.12	0.078
			C_2	RY*(1)	0.00818	3.01	2.10	0.072
			C_2	RY*(2)	0.00586	1.65	2.84	0.062
			C_5	RY*(1)	0.00644	4.81	1.76	0.083
O_6	LP_2	1.6370	C_2-C_3	π *	0.3967	43.07	0.41	0.119
			C_2	RY*(3)	0.00379	4.56	1.49	0.081
			C_1-C_2	σ *	0.03466	1.94	1.20	0.043
			C_4-C_5	π *	0.31739	46.65	0.38	0.120
N_7	LP_1	1.9135	C_1-H_{12}	σ *	0.0368	10.17	0.75	0.079
			N_8-C_9	σ *	0.0717	1.01	0.84	0.026
			C_1	RY*(1)	0.00689	5.14	1.47	0.079
			C_1-C_2	σ *	0.03466	3.24	1.01	0.052
			N_8-H_{16}	σ *	0.03387	8.68	0.75	0.073
N_8	LP_1	1.70147	C_1-N_7	π *	0.27638	31.59	0.28	0.085
			C_9-O_{10}	π *	0.37858	52.61	0.30	0.115
O_{10}	LP_1	1.98006	N_8-C_9	σ *	0.07177	1.29	1.12	0.034
			C_9-N_{11}	σ *	0.06431	1.47	1.12	0.037
O_{10}	LP_2	1.8563	N_7-N_8	σ *	0.0238	0.90	0.63	0.022
			N_8-C_9	σ *	0.0717	24.22	0.68	0.117
			C_9-N_{11}	σ *	0.0643	23.54	0.69	0.116
			N_{11}-H_{18}	σ *	0.0116	0.64	0.66	0.019

ED Electron Density

[a] $E^{(2)}$ means energy of hyper conjugative interaction (stabilization energy).

[b] Energy difference between donor and acceptor i and j NBO orbitals.

[c] F(i,j) is the Fock matrix element between i and j NBO orbitals.

The results of second order perturbation theory analysis of Fock matrix at B3LYP/6-31++G(d,p) level of theory are collected in Table 5. The strong intramolecular hyperconjugative interaction of the σ and π electrons of the C-C, C-O, C-H and C-N to the anti C-C, C-O, C-H and N-H bond of the furan ring as well as the semicarbazone group leads to stabilization of some part of the ring. The intermolecular hyper conjugation interaction of the σ(C_1-C_2), distributed to σ*(C_2-O_6) (C_1-N_7), (C_2-C_3) leads to stabilization of approximately 3.3. 4.1 and 7.2 kJ/mol. furthermore, π(C_1-N_7) NBO conjugates with the anti-bonding orbitals of π^*(C_2-C_3) which lead to strong delocalization of 13.37 kJ/mol. The LP_2(O_6) of NBO conjugated with the π^*(C_2-C_3) results in a high stabilization of 43.07 kJ/mol. These interactions are observed as increase in Electron Density (ED) in C-C, C-N, anti-bonding orbital that weakens the respective bonds. The energies for the interaction $LP_1(O_6)\rightarrow\sigma^*(C_4\text{-}C_5)$ and $LP_1(N_7)\rightarrow\sigma^*(C_1\text{-}H_{12})$ are 6.66 and 10.17 kJ/mol, respectively, which clearly demonstrate that the intermolecular hyper conjugative interaction between the semi carbazone group is strong in the ground state. There occurs a strong intermolecular hyperconjugative interaction of (C_2-C_3) from O_6 (LP_2 (O_6) → π^*(C_2-C_3) which increases ED (0.3967 eV) that weakens the respective bonds (C_2-C_3) leading to stabilization of 43.07 kJ/mol. These charge transfer interactions of FSC are responsible for pharmaceutical and biological properties. Hence, the FSC structure is stabilized by these orbital interactions.

Frontier Molecular Orbital Analysis

Molecular orbitals (HOMO and LUMO) and their properties such as energy are very useful for physicists and chemists and are very important parameters for quantum chemistry. This is also used by the frontier electron density for predicting the most reactive position in π- electron systems and also explains several types of reaction in conjugated system.

Table 6 Selected HOMO and LUMO energies of FSC

S.no	Molecular orbital (eV)	B3LYP/ 6-31++G(d,p)	B3LYP/ 6-311++G(d,p)
1.	E_{HOMO}	-6.0402	-6.0913
2.	E_{HOMO-1}	-7.5218	-7.5825
3.	E_{HOMO-2}	-7.5256	-7.5887
4.	E_{LUMO}	-1.7307	-1.7627
5.	E_{LUMO+1}	-0.3679	-0.3689
6.	E_{LUMO+2}	-0.0822	-0.0849
7.	$\Delta E_{(HOMO-LUMO)}$	4.3095	4.3285
8.	$\Delta E_{(HOMO-1-LUMO)}$	5.7911	5.8197
9.	$\Delta E_{(HOMO-2-LUMO)}$	5.7949	5.8260
10.	$\Delta E_{(HOMO-LUMO+1)}$	5.6722	5.7223
11.	$\Delta E_{(HOMO-1-LUMO+1)}$	7.1539	7.2135
12.	$\Delta E_{(HOMO-2-LUMO+1)}$	7.1577	7.2197
13.	$\Delta E_{(HOMO-LUMO+2)}$	5.9579	6.0064
14.	$\Delta E_{(HOMO-1-LUMO+2)}$	7.4396	7.4976
15.	$\Delta E_{(HOMO-2-LUMO+2)}$	7.4434	7.5038

The electronic absorption corresponds to the transition from the ground to the first excited state and is mainly described by one electron excitation from the highest occupied molecular orbital (HOMO) to the lowest unoccupied molecular orbital (LUMO). Commonly the atom occupied by more densities of HOMO should have stronger ability for detaching electrons, whereas the atom with more occupation of LUMO should be easier to gain electrons Ravi Kumar et al (2008), Dixon et al (2003). The atomic orbital compositions of the frontier molecular orbital are shown in Figure 5.

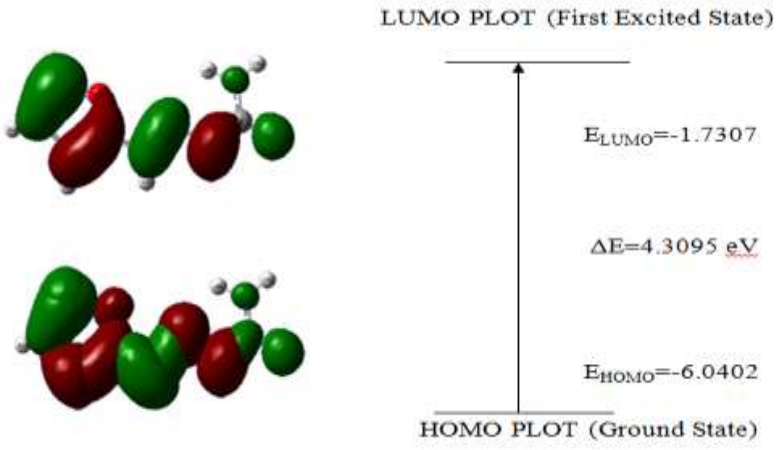

Figure 5 Molecular orbital surface Figure for the HOMO and LUMO of FSC

In order to evaluate the energetic behaviour of the title molecule, the energies of HOMO, LUMO and their orbital energy gaps using B3LYP/6-31++G(d,p) and 6-311++G(d,p) basis sets are calculated and presented in Table 6. The HOMO lying at -6.0402 eV is delocalized over π orbital and includes mixing of lone pairs of electrons on all the oxygen as well as nitrogen atoms. The H-1 at-7.5218 eV below the HOMOs is localized over nitro group through the furan ring. The H-2 at -7.5256 eV below the HOMO and has mainly of π bonding character along with some sigma bond character, whereas the LUMO lying at-1.7307 eV is a π^* orbital, delocalized over the entire molecule with large anti-bonding character from Table 1.6. It is evident that the absorption band centered around arises mainly due to the four electronic transitions given by H→L, H-1→L, H-2→L,H→L+1, H-1→L+1, H-2→L+1, H→L+2, H-1→L+2, H-2→L+2. Are assigned as π-π^* type whereas the more intense band around 312 nm, having maximum oscillator strength (0.567), corresponds to H→L transition and is

mainly characterized to the $LP_2 \rightarrow \pi^*$ type. The higher intensity of band corresponding to the $LP_2 \rightarrow \pi^*$ type transition is attributed to the presence of large number of free lone pairs of electrons available on two oxygen and three nitrogen atoms. It can be seen from the plots that the HOMO is spread over the entire molecule and shows appreciable amount of π bonding character. The LUMO is also found to be uniformly distributed over the molecule and reflects a lot of anti-bonding π character. The energy gap of HOMO-LUMO explains the eventual charge transfer interaction within the molecule, and the frontier orbital energy gap in case of FSC is found to be 4.3095 eV obtained at B3LYP/6-31++G(d,p) method.

Fukui Function

The hard and soft acids and bases principle has been used in a local sense in terms of DFT concepts such as the Fukui function of f(r). Pared Yang showed that sites in chemical species with the largest values of Fukui function f(r) are those with higher reactivity. The Fukui function is defined as Huizar et al (2011):

$$F(r) = [\delta\rho(r)/\delta N]_\upsilon \quad (3)$$

Where $\rho(r) \rightarrow$electronic density,

$N \rightarrow$ number of electrons.

The Fukui function is a local reactivity descriptor that indicates the preferred regions where a chemical species will change its density when the number of electrons is modified.

Therefore, it indicates the property of the electronic density to deform at a given position upon accepting (or) donating electrons Roy et al (1999) and also it is possible to define the corresponding condenses or atomic fukui functions on the j^{th} atom site as;

$$f_k^- = q_k(N) - q_k(N-1) \quad (4)$$

$$f_k^+ = q_k(N+1) - q_k(N) \quad (5)$$

$$f_k^o = \tfrac{1}{2}[q_k(N+1) - q_v(N-1)] \quad (6)$$

For an electrophilic $f_k^-(r)$, nucleophilic $f_k^+(r)$ and free radical attack $f_k^o(r)$, on the references molecule, respectively. In these equation, q_k is the atomic charge (evaluated from Mulliken population analysis, electrostatic derives charge, etc.) at the k^{th} atomic site in the neutral (N), anionic (N+1) or cationic (N-1) chemical species. Hence, it is important to mention q_k independently of the approximations used for calculation.

$$\int f(r)\, dr = 1 \quad (7)$$

The condensed Fukui functions and condensed local softness indices allow us to distinguish each part of the molecule on the basis of its distinct chemical behaviour due to the different substituent functional groups. Thus, the site for nucleophilic attack will be the place where the value of $\int f(r)\, dr = 1$ for nucleophilic attack in the most reactive site of FSC is on the O_{10} and C_3 atoms respectively. For electrophilic attack the most reactive site of FSC is on the C_5 and C_1 respectively. These results are shown in Table 7. The condensed local softness indices Sf_k^- and Sf_k^+ are related to the condensed Fukui functions. The local softness also follows the same trend to fukui functions.

Table 7 Condensed Fukui functions calculated by B3LYP/6-311++G(d,p) of FSC

Atoms	f_k^+	f_k^-	f_k^0	Sf_k^+	Sf_k^-	Sf_k^0
C_1	0.0081	0.1964	0.1022	0.0019	0.0456	0.0237
C_2	-0.0047	-0.1356	-0.0701	-0.0011	-0.0315	-0.0163
C_3	0.1180	0.1436	0.1308	0.0274	0.0333	0.0304
C_4	0.0246	-0.0661	-0.0207	0.0057	-0.0153	-0.0048
C_5	0.0868	0.2383	0.1626	0.0201	0.0553	0.0377
O_6	0.0430	0.0107	0.0269	0.0100	0.0025	0.0062
N_7	0.0815	0.1157	0.0986	0.0189	0.0268	0.0229
N_8	0.0893	-0.0290	0.0302	0.0207	-0.0067	0.0070
C_9	-0.0175	0.0014	-0.0081	-0.0041	0.0003	-0.0019
O_{10}	0.1299	0.0899	0.1099	0.0301	0.0209	0.0255
N_{11}	0.0275	0.0196	0.0235	0.0064	0.0046	0.0055
H_{12}	0.0695	0.0843	0.0769	0.0161	0.0196	0.0178
H_{13}	0.0786	0.0816	0.0801	0.0182	0.0189	0.0186

H_{14}	0.0762	0.0744	0.0753	0.0177	0.0173	0.0175
H_{15}	0.0830	0.0765	0.0797	0.0193	0.0178	0.0185
H_{16}	0.0567	0.0567	0.0567	0.0132	0.0132	0.0132
H_{17}	0.0389	0.0411	0.0400	0.0090	0.0095	0.0093
H_{18}	0.0105	0.0005	0.0055	0.0024	0.0001	0.0013

CONCLUSION

In this study the spectroscopic properties such as molecular parameters, frequency assignments and structural confirmation of title compound are examined by using FT-IR, FT-Raman and tools derived from the DFT. The optimized geometric parameters (bond length and bond angles) were theoretically determined B3LYP/6-31++G(d,p) and 6-311++(d,p) levels of theory and compared with the structurally similar compounds. The vibrational FT-IR and FT-Raman spectra of FSC were recorded and computed vibrational wave numbers and their PED were calculated. When all theoretical results are scanned, they are showing good correlation with experimental data. The differences between the observed and scaled wave number values of most of the fundamentals are very small. Therefore, the assignments made at DFT level of theory with only reasonable deviations from the experimental values seem to be correct. NBO analysis is made and it is indicating the intra-molecular charge transfer between bonding and antibonding orbitals. The bond order and atomic charges of the title molecule have been studied by DFT methods. Charge transfer occurs in the molecule between HOMO and LUMO energies, and Frontier energy gap is calculated and presented. The lowering of the HOMO-LUMO energy gap value has substantial influence on the intra-molecular charge transfer and bioactivity of the molecule. Fukui function helps to identify the electrophilic*/* nucleophilic nature of a specific site within a molecule.

REFERENCES

1. Becke, AD 1993, 'Density-Functional Thermo chemistry. III. The Role of Exact Exchange', J. Chem. Phys, vol. 98, pp. 5648-5652.
2. Pulay, P, Fogarasi, G, Pongar, G, Boggs, JE & Vargha, A 1983, 'Combination of theoretical ab initio and experimental information to obtain reliable harmonic force constants – scaled quantum-mechanical (SQM) force fields for glyoxal, acrolein, butadiene, formaldehyde and ethylene', J.Am. Chem.soc, vol.105, pp.7037-7047.
3. Fogarasi, G, Pulay, P & During, JR 1985, 'Ab initio Calculation of Force Fields and Vibrational Spectra, in: Vibrational Spectra and Structure', ed. J. R. Durig (Elsevier, Amsterdam), vol.14, pp.125-219.
4. Sundius, T 2002, 'Scaling of ab initio force fields by MOLVIB', Vib. Spectrosc, vol. 29, pp. 89–95.
5. Lee, C, Yang, W & Parr, RG 1988, 'Development of the Colle-Salvetti conelation energy formula into a functional of the electron density', Phys. Rev, vol. B 37, pp. 785-789.
6. Olszak, TA, Peteres, OM, Blaton, NM & De Ranter CJ 1995, '5-Nitro-2-furaldehyde semicarbazone', Acta Crystalogr, vol. C51, pp.1304-1306.
7. Keresztury, G, Chalmers, JM & Griffiths, PR 2002, 'Raman Spectroscopy; Theory in Handbook of Vibrational Spectroscopy'. John Wiley and Sons Ltd, vol.17.
8. Glendening, ED, Reed, AE, Carpenter, JE & Weinhold, F 1998, 'Introduction to Infrared and Raman Spectroscopy', NBO Version 3.1. TCI, University of Wisconsin, Madison.
9. Klots, TD, Chirico, RD & Steele, WV 1994, 'Complete vapor phase assignment for the fundamental vibrations of furan, pyrrole and thiophene', Spectrochimica Acta Part A, vol. 50, no.4, pp.765-795.
10. Bambagiooti, M, Castellucci, E & Sbrana, G 1974, 'Vibrational spectra and crystal structure of 2, 2'-bifurane', Spectrochimica Acta Part A, vol.30, pp.1413-1424.
11. Zinczuk, J, Ledasma, AE, Brandhan, SA, Piro, OE, Gonzalez, JJL & Atabef, AB 2009, 'Structural and vibrational study of 2-(2′- furyl)-4, 5-1 *H*-dihydroimidazole', J Phy Org Chem, vol.22, no.12, pp.1166–1177.
12. Rastogi, VK, Palafox, MA, Tanwar, RP & Mittal, L 2002, '3, 5-Difluorobenzonitrile: Ab initio calculations, FTIR and Raman spectra', Spectrochim. Acta, vol. A58, no.9, pp. 1987–2004.
13. Arivazhagan, M, Sambath Kumar, K & Jeyavijan, S 2010, 'Density functional theory study of FT-IR and FT-Raman spectra of 7-acetoxy-4-methyl coumarin', Indian J pure & Appl Phys, vol. 48, no. 10, pp. 716-722.
14. Zhang, R, Du, B, Sun, G & Sun, YX 2010, 'Experimental and theoretical studies on o-, m- and p-chlorobenzylidene aminoantipyrines', Spectrochim. Acta, vol. 75, pp. 1115-1124.

15. Silverstein, RM & Webster, FX 2003, 'Spectrometric Indentifition of Organic compounds', Sixth edu (John wiley, Inc, New York).

16. Dani, VR 1995, 'Organic spectroscopy', Tata-McGraw Hill publishing Company, New Delhi, pp. 86-168.

17. Socrates, G 2001, 'Infrared and Raman characteristic group frequencies- Tables and Charts, wiley, Chichester'.

18. Reed, AE, Curtiss, LA & Weinhold, F 1988, 'Intermolecular Interactions from a Natural Bond Orbital, Donor-Acceptor Viewpoint', Chem Rev, vol.88, pp.899-926.

19. Choo, J, Kim, S, Joo, H & Kwon, Y 2002, 'Molecular structures of (trifluoromethyl) iodine dihalides CF3IX2 (X=F, Cl): ab initio and DFT calculations', J. mol.struct. (Theochem), vol. 587, pp 1-8.

20. Luque, FJ, Lopez, JM & Orozco, M 2000, 'Perspective on Electrostatic interactions of a solute with a continuum. A direct utilization of ab initio molecular potentials for the prevision of solvent effects, Theory' Chem. Acc, vol.103, pp.343-345.

21. Okulik, N & Jubert, AH 2005, 'Theoretical Analysis of the Reactive Sites of Non–steroidal Anti–inflammatory Drugs', Internet Electr. J. Mol. Des, pp.4–17.

22. Ravi Kumar, C, Joe, IH & Jaya Kumar, VS 2008, 'Charge transfer interactions and nonlinear optical properties of push–pull chromophore benzaldehyde phenylhydrazone: A vibrational approach', Chem Phys Lett, vol. 460, pp. 552-558.

23. Dixon, A, David, Chang-Guo Zhan, Jeffrey, A & Nicholas 2003, 'Ionization Potential, Electron Affinity, Electrone gativity, Hardness, and Electron Excitation Energy: Molecular Properties from Density Functional Theory Orbital Energies', J-Phys-Chem., vol. A.107, and pp. 4184-4195.

24. Huizar, LH, Mendoza & Reyes Clara, HR 2011, 'Chemical Reactivity of Atrazine Employing the Fukui Function, J. Mex. Chem. Soc', vol. 55, no.3, pp.172-184.

25. Roy, RK, Pal, S & Hirao, K 1999, 'On Non-Negativity of Fukui Function Indices', J. Chem. Phys, vol.110, pp.8236-8245.